Geophysical Journal International

Geophys. J. Int. (2011) **186,** 980–986 doi: 10.1111/j.1365-246X.2011.05091.x

GJI Geomagnetism, rock magnetism and palaeomagnetism

New analytic solutions for the 2-D TE mode MT problem

Robert L. Parker

Institute of Geophysics and Planetary Physics Scripps Institution of Oceanography University of California, San Diego, CA 92093-0225, USA. E-mail: rlparker@ucsd.edu

Accepted 2011 May 22. Received 2011 May 13; in original form 2010 November 1

SUMMARY

A closed-form solution is given for a 2-D, transverse electric mode, magnetotelluric (MT) problem. The model system consists of a finite vertical thin conductor with variable integrated conductivity over a perfectly conducting base. A notable property of the solution is that the frequency response possesses a single pole in the complex plane. Systems with finitely many resonances play a central role in the 1-D MT inverse problem based on finite data sets, but until now, no 2-D system of this kind was known. The particular model is shown to be just one of a large class of thin conductors with same the property, and further examples are given. The solutions of the induction problem for members of this family can often be written in compact closed form, making them the simplest known solutions to the 2-D MT problem.

Key words: Electromagnetic theory; Magnetotelluric; Geomagnetic induction.

1 INTRODUCTION

In the 1-D inverse problem of magnetotelluric (MT) sounding based on a finite set of response observations, one encounters conductivity profiles with only a finite number of resonances in their response functions (Parker & Whaler 1981). The resonances of a physical system correspond to singularities in its frequency response; because the fields in the MT problem obey a diffusion equation, the resonant frequencies are not real, but are located on the imaginary axis of the complex frequency plane. Sturm-Liouville theory Parker (1994) shows in the 1-D case that every positive conductivity function with bounded integral must be associated with infinitely many imaginary resonances which correspond to eigenvalues of the differential operator. Therefore systems with a finite set must be singular is some way, and the electrical profile with this behavior comprises a sum of delta functions in conductivity. In two or three dimensions, we expect on the basis of a finite difference approximation that systems of bounded conductivity in compact regions will also be associated with infinitely many imaginary resonances, although the author is unaware of a rigorous proof. The question naturally arises, Are there any singular conductivity distributions in higher dimensions associated with a finite set of resonances?

We concentrate on the 2-D transverse electric MT problem. Motivated by analogy with the 1-D situation, we study initially a thin conducting strip, oriented vertically, with variable integrated conductivity. We find a particular conductivity distribution yields a very simple analytic solution with a single, purely imaginary, resonance in its frequency response. That solution possesses two other unusual properties, an observation that prompts an investigation of other possible models with one of them, namely, that the electric field in the conductor can be written as the product of a function of position and a function of frequency, a kind of separation of variables.

We discover a large class of models comprised of thin conductors with longitudinal conductivity variation that share this property. We show they also exhibit a single resonant frequency. Several explicit examples are given, which we derive from solutions to Laplace's equation using complex variable theory, although other techniques can be equally effective. These new results appear to be the simplest complete solutions to a 2-D MT problem currently known.

2 THE THIN CONDUCTOR

The first physical system to be studied comprises a thin vertical conducting ribbon of length a with its lower end resting on a perfectly conducting half-space with boundary $z = 0$; Fig. 1. It could be a primitive model for a dike intruded into a sedimentary matrix or a mid-oceanic rise. We choose coordinates with $z > 0$ upwards, y along the ribbon, which is infinite in both directions since this is a 2-D problem. The electrical conductivity varies with z: we assume the conductance function

$$\tau(z) = \int_{-d/2}^{d/2} \sigma(x, z)\mathrm{d}x, \quad 0 \le z < a \tag{1}$$

which remains finite, as the thickness d tends zero and σ grows without bound. An externally generated, time-periodic, spatially uniform magnetic field in the form $\mathbf{B_0} = \hat{\mathbf{x}} B_0 \mathrm{e}^{\mathrm{i}\omega t}$ drives electromagnetic induction in the system; we will refer to ω as the frequency. This is transverse electric, or TE, mode induction (Weaver 1994). We will assume observations of electric and magnetic fields can be made on the line $z = h$ with $h < a$.

We ignore displacement currents in an idealized model, even in the high frequency limit, where this approximation would obviously

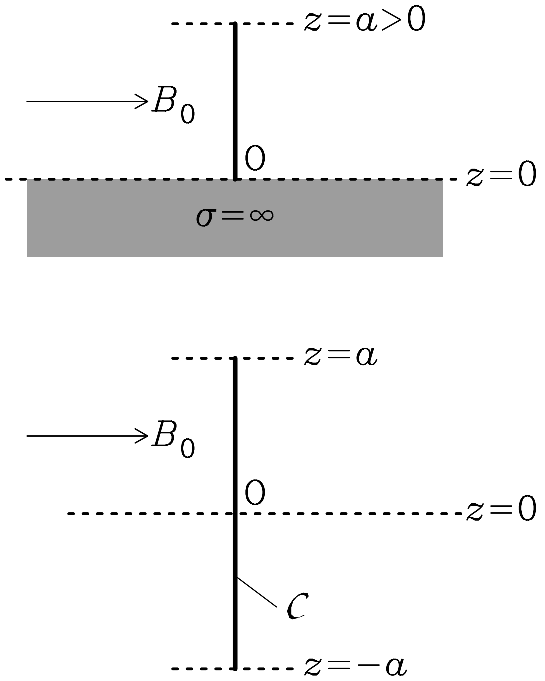

Figure 1. Top: the physical system of a thin conducting ribbon over a perfect conductor. Bottom: equivalent system in which an image conductor replaces the perfect conductor.

fail for a physical system. We solve for E_y, the y component of the electric field. In TE mode induction $\nabla^2 E_y = \mathrm{i}\omega\mu_0\sigma E_y$ and the other components of $\mathbf{E}$ vanish. Away from the conductors, $\nabla^2 E_y = 0$. The perfect conductor at the base provides the boundary condition on $z = 0$ that $\hat{\mathbf{z}} \cdot \mathbf{B} = -\partial E_y/\partial x = 0$; far from the origin $E_y \to \mathrm{i}\omega B_0 z$. We can satisfy the first boundary condition by replacing the basement conductor with an image of the ribbon, as shown in Fig. 1. We perform our calculations in the equivalent model, where the extended thin conductor is called $\mathcal{C}$. Now the system exhibits the symmetry $E_y(x, z) = -E_y(x, -z)$ and so the magnetic field of the currents in $z < 0$ cancel vertical magnetic fields on $z = 0$ as we require. The tangential component of $\mathbf{B}$ is discontinuous across $\mathcal{C}$ but B_n, the normal magnetic field, is continuous. We relate B_n to $\mathbf{E}$ with Faraday's law

$$\hat{\mathbf{x}} \cdot \nabla \times \mathbf{E} = -\mathrm{i}\omega\hat{\mathbf{x}} \cdot \mathbf{B} = -\mathrm{i}\omega(B_0 + \hat{\mathbf{x}} \cdot \mathbf{B}_J), \tag{2}$$

where $\mathbf{B}_J$ is the magnetic field due to induced currents in $\mathcal{C}$. Applying Ohm's law and the Biot-Savart formula to (2) we obtain

$$-\frac{\mathrm{d}E}{\mathrm{d}z} = -\mathrm{i}\omega\left[B_0 - \frac{\mu_0}{2\pi}\int_{-a}^{a}\frac{\tau(z')E(z')}{z'-z}\mathrm{d}z'\right], \tag{3}$$

where $E(z) = E_y(0, z)$; the principal part of the integral is understood. By integrating over z and exploiting the z symmetry we obtain a Fredholm integral equation of the second kind for E on $\mathcal{C}$

$$E(z) = \mathrm{i}\omega B_0 z - \frac{\mathrm{i}\omega\mu_0}{2\pi}\int_0^a \ln\left|\frac{z'+z}{z'-z}\right|\tau(z')E(z')\,\mathrm{d}z', \quad 0 \le z \le a. \tag{4}$$

There are several ways to solve this kind of equation in addition to purely numerical techniques (Porter & Stirling 1990). For our purposes the spectral expansion, or Hilbert–Schmidt method, applied after symmetrizing the kernel, has the advantage of exposing the frequency behavior of the solution. By comparison with the case $\tau = 1$, it can be shown (Porter & Stirling 1990,Chapter 7) that when τ is positive and bounded, the kernel in (4) has infinitely many real, positive eigenvalues, and thus there are an infinite number of purely imaginary resonances for E. This means that τ must be singular in some way to achieve our goal.

3 A SINGULAR CONDUCTANCE FUNCTION

We introduce the singular conductance function

$$\tau(z) = \frac{a\tau_0}{\sqrt{a^2 - z^2}}, \quad |z| < a. \tag{5}$$

To solve (4) with this profile in terms of elementary functions we make a change of variables: let $z = a\cos\phi$ and $z' = a\cos\psi$; then (4) becomes

$$f(\phi) = \cos\phi - \mathrm{i}\Omega\int_0^{\pi/2}\ln\left|\frac{\cos\psi + \cos\phi}{\cos\psi - \cos\phi}\right| f(\psi)\mathrm{d}\psi, \tag{6}$$

where $\Omega = \omega\mu_0\tau_0 a/2\pi$, a dimensionless frequency which is the sole parameter governing the system, and

$$f(\phi) = \frac{E(a\cos\phi)}{\mathrm{i}\omega a B_0}. \tag{7}$$

Following the treatment of a similar problem by Porter and Stirling (Example 7.8, 1990), we invoke the Hilbert–Schmidt methodology. Consider the eigensystem

$$Ku_n = \lambda_n u_n, \quad n = 1, 2, \ldots, \tag{8}$$

where

$$Kf = \int_0^{\pi/2}\ln\left|\frac{\cos\psi + \cos\phi}{\cos\psi - \cos\phi}\right| f(\psi)\mathrm{d}\psi. \tag{9}$$

The Fourier series expansion

$$\ln\left|\frac{\cos\psi + \cos\phi}{\cos\psi - \cos\phi}\right| = \sum_{n=1}^{\infty}\frac{4}{2n-1}\cos(2n-1)\psi\cos(2n-1)\phi \tag{10}$$

shows that the eigensystem (8) is satisfied by

$$\lambda_n = \frac{\pi}{2n-1}; \quad u_n(\phi) = \frac{2}{\sqrt{\pi}}\cos(2n-1)\phi. \tag{11}$$

This family of eigenfunctions is complete in $L_2(0, \frac{1}{2}\pi)$ and orthonormal. It follows that we can expand the solution to (6) in the basis

$$f(\phi) = \sum_{n=1}^{\infty}\alpha_n u_n(\phi) \tag{12}$$

which, upon substitution into the integral equation, leads to exactly one nonzero coefficient, namely, $\alpha_1 = \frac{1}{2}\sqrt{\pi}/(1 + \mathrm{i}\pi\Omega)$. Thus by (11) and (12)

$$f(\phi) = \frac{\cos\phi}{1 + \mathrm{i}\pi\Omega} \tag{13}$$

from which we conclude that

$$E(z) = \frac{\mathrm{i}\omega B_0 z}{1 + \mathrm{i}\pi\Omega} = \frac{\mathrm{i}\omega B_0 z}{1 + \frac{1}{2}\mathrm{i}\omega\mu_0\tau_0 a}, \quad |z| < a. \tag{14}$$

The current density and normal magnetic field are:

$$j(z) = \tau(z)E(z) = \frac{\mathrm{i}\omega a\tau_0 B_0}{1 + \mathrm{i}\pi\Omega}\frac{z}{\sqrt{a^2 - z^2}}, \quad |z| < a \tag{15}$$

$$B_n(z) = \frac{B_0}{1 + \mathrm{i}\pi\Omega}, \quad |z| < a. \tag{16}$$

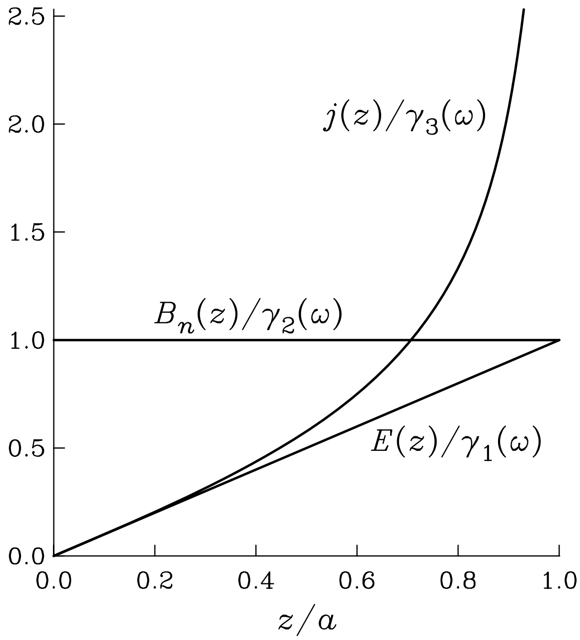

Figure 2. Dimensionless E, j, and B_n on the conductor $\mathcal{C}$. Here $\gamma_1 = \mathrm{i}\omega B_0/(1 + \mathrm{i}\pi\Omega)$; $\gamma_2 = B_0/(1 + \mathrm{i}\pi\Omega)$; $\gamma_3 = \mathrm{i}\omega a \tau_0 B_0/(1 + \mathrm{i}\pi\Omega)$.

The solutions for E, j and B_n possess a single resonant frequency at $\omega = 2\mathrm{i}/\mu_0\tau_0 a$. Another unusual aspect is the fact that on $\mathcal{C}$ (though not elsewhere, as we will see) these fields retain the same geometrical form whatever the frequency; Fig. 2. A third peculiarity is that each term in (4) is proportional to the same function, z. We will show that these three properties are related. But first we will extend the solution from the ribbon into the whole domain and thus obtain the MT frequency response.

4 THE FREQUENCY RESPONSE

In practice the MT response of a geological system is found from a ratio of the horizontal electric and magnetic fields at sites on the Earth's surface, which would be a horizontal line above the ribbon. Eq. (14) gives the electric field only on $\mathcal{C}$, so we need to calculate B_x and E_y for points with $x \neq 0$ and $z > a$. Although we restricted z to be less than a in (4) for the purpose of setting up an integral equation, the equation remains valid for $z > a$ as well. So first we to compute the electric field on the remainder of the z-axis using (4). Inserting (5) and (14) we find:

$$\frac{E(z)}{\mathrm{i}\omega B_0} = z - \frac{\mathrm{i}\Omega}{1 + \mathrm{i}\pi\Omega} \int_0^a \ln\left|\frac{z' + z}{z' - z}\right| \frac{z'}{\sqrt{a^2 - z'^2}}\, \mathrm{d}z', \quad |z| > a \tag{17}$$

$$= z - \frac{\mathrm{i}\pi\Omega}{1 + \mathrm{i}\pi\Omega}\left(z - \sqrt{z^2 - a^2}\right). \tag{18}$$

Eqs (14) and (18) can be combined into a single equation that gives E_y everywhere on the z-axis

$$\frac{E_y(0, z)}{\mathrm{i}\omega B_0} = z - \frac{\mathrm{i}\pi\Omega}{1 + \mathrm{i}\pi\Omega}\left(z - \mathrm{Re}\sqrt{z^2 - a^2}\right). \tag{19}$$

Recall that the electric field E_y surrounding $\mathcal{C}$ is harmonic because in general $\nabla^2 E_y = \mathrm{i}\omega\mu_0\sigma E_y$ and $\sigma = 0$ outside $\mathcal{C}$. So E_y can be expressed in terms of an analytic function of a complex coordinate $\zeta = x + \mathrm{i}z$, Needham (1999). Suppose we write

$$\frac{E_y(x, z)}{\mathrm{i}\omega B_0} = z - \frac{\mathrm{i}\pi\Omega}{1 + \mathrm{i}\pi\Omega} \mathrm{Re}\, g(x + \mathrm{i}z). \tag{20}$$

To find g we focus on the behavior on the imaginary axis; we make the identification that $\mathrm{Re}\, g(\mathrm{i}z) = z - \mathrm{Re}\sqrt{z^2 - a^2}$, which when $\zeta = \mathrm{i}z$ suggests

$$g(\zeta) = \mathrm{i}\sqrt{\zeta^2 + a^2} - \mathrm{i}\zeta. \tag{21}$$

With a straight branch cut running between $\pm\mathrm{i}a$ on the top sheet, if the positive sign is taken for the square root with real ζ, g tends to zero for large $|\zeta|$. Then it can be verified that on the imaginary ζ axis (20) agrees with (19) on the z axis, and also matches E_y far from the origin. By a uniqueness theorem for Laplace's equation (Kellogg 1953,chap VIII) two harmonic functions that agree on a boundary enclosing a region must be identical within: so (20) with (21) is identical to E_y everywhere.

Eq. (20) provides a convenient way to compute the electric field in the system. The magnetic fields are readily found by taking the curl

$$\frac{B_x(x, z)}{B_0} = 1 + \frac{\mathrm{i}\pi\Omega}{1 + \mathrm{i}\pi\Omega} \mathrm{Im}\, g'(x + \mathrm{i}z) \tag{22}$$

$$\frac{B_z(x, z)}{B_0} = \frac{\mathrm{i}\pi\Omega}{1 + \mathrm{i}\pi\Omega} \mathrm{Re}\, g'(x + \mathrm{i}z), \tag{23}$$

where

$$g'(\zeta) = \frac{\mathrm{d}g}{\mathrm{d}\zeta} = \frac{\mathrm{i}\zeta}{\sqrt{\zeta^2 + a^2}} - \mathrm{i}. \tag{24}$$

Notice that the functions in (20), (22) and (23) are not analytic functions in the complex ζ plane. The fields are illustrated in Fig. 3 for the parameter $\Omega = 1/\pi$. These plots may also interpreted as magnetic field lines.

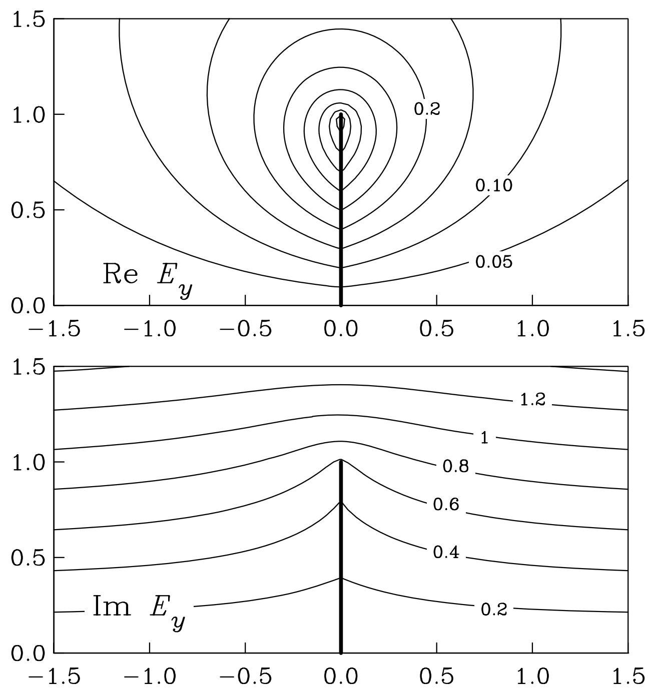

Figure 3. Contours of $E_y/a\omega B_0$ for $\Omega = 1/\pi$. Distances scaled by a. The field E_y is the stream function for $\mathrm{i}\omega\mathbf{B}$, and so level lines of E_y are lines of force for $\mathbf{B}$ with real and imaginary parts interchanged.

Now we can calculate the c frequency response (the admittance) at a site with coordinates (x, z)

$$c(\omega, x, z) = \frac{E_y}{\mathrm{i}\omega B_x} = \frac{z + \mathrm{i}\pi\Omega[z - \mathrm{Re}\, g(x + \mathrm{i}z)]}{1 + \mathrm{i}\pi\Omega[1 + \mathrm{Im}\, g'(x + \mathrm{i}z)]}. \quad (25)$$

We see from this expression that $c(\omega)$ also has a single pole on the imaginary axis in the complex ω plane, but it is not generally at $\Omega = \mathrm{i}/\pi$: the resonant frequency for c varies with the location of the measurement. One would expect there to be a single resonance for the physical system independent of position. This is so if the frequency response is defined with respect to the driving field B_0, but traditionally in MT one uses the *local* magnetic field $B_x(x, z)$ at each site as though it were the source term in constructing responses like $c(\omega)$ or $Z(\omega)$.

5 AN ALTERNATIVE DERIVATION

At the end of Section 3 we remarked that the solution obtained for the conductance model given in (5) exhibits three unusual attributes including that of a possessing a single resonance. We will show that the three properties are related and that a large class of models share them. We focus on the characteristic that the current density and fields in the thin conductor always have the same geometrical form independent of frequency, and we look for a conductance function τ that is consistent with that condition.

Let us write (4) compactly as

$$e = \mathrm{i}\omega[f - K(\tau e)], \quad (26)$$

where K is the integral operator derived from the Bio-Savart law, and τ is the real, positive conductance function, unknown at this point, and $\mathrm{i}\omega f$ is the electric field associated with the external magnetic field $\mathbf{B}_0$. In the limit of infinite frequency, the factor in brackets must tend to zero, expressing the fact that the normal magnetic field at the surface of the strip vanishes when the source field is exactly canceled by the one generated by induced currents. The infinite-frequency E_y in the conductor remains finite, as the solution in (14) illustrates. The corresponding current density can found from the solution to the Fredholm equation of the first kind

$$K(j_*) = f. \quad (27)$$

The function f and hence j_* will generally be real valued and it depends only on the shape of the thin conductor. By means of the Hilbert–Schmidt process we can solve (27)

$$j_*(z) = \frac{2B_0 z}{\mu_0\sqrt{a^2 - z^2}}. \quad (28)$$

Now we seek a solution for e at finite ω which has the same geometrical form as f for all frequencies: in other words, it can be written as the product of two factors, one depending on frequency only, the other, f, on position only

$$e(z, \omega) = \beta(\omega) f(z). \quad (29)$$

Here β may be complex. Inserting (29) into (27) we infer that

$$\varpi K(\tau f) = f, \quad (30)$$

where $\varpi = \beta(\infty)$. We observe ϖ is real. Substituting (29) and (30) into (26) we find

$$\beta(\omega) = \frac{\mathrm{i}\omega}{1 + \mathrm{i}\omega/\varpi}. \quad (31)$$

Hence we see that the condition of geometrical similarity automatically yields a single resonant frequency, and that frequency is $\mathrm{i}\varpi$.

Since f is known we can solve for the conductance by looking at the infinite-frequency limit

$$\tau(z) = \frac{j_*(z)}{\varpi f(z)} = \frac{2}{\mu_0 \varpi\sqrt{a^2 - z^2}} \quad (32)$$

from (28), which agrees with (5) when $\varpi = 2/\mu_0 a \tau_0$. Eq. (32) cannot yield a physical conductance if the ratio of f and j_* changes sign on the interval $(0, a)$, but of course for the system we have chosen this presents no difficulty. This derivation has generated a family of conductivity models, related to each other by a multiplicative factor, the constant ϖ, a free parameter setting the scale for the conductance.

In the foregoing analysis we have assumed a particular geometry for the conducting sheet and by means of the factorization (29) we have deduced the conductance in a kind of inverse problem. The analysis does not in fact rely on the particular shape of the thin conductor, and it can be applied to 2-D thin sheets of almost any shape as we will discuss next.

6 GENERALIZATION: THE CLASS SR^+

Suppose that (26) applies to a thin sheet with a completely different shape from that of our particular example. Then K will be different in detail from the kernel in (4); in fact it must now be a line integral on the possibly curved conductor, and it will always be real. The function f is found by integrating the normal component of $\mathbf{B}_0$ along the conductor; it is easily seen that $f(s) = z(s)B_0$, where s is the distance along the conductor. In the limit of infinite frequency, currents flow to cancel the normal magnetic field and so j_* can be discovered by solving (27). We may interpret the infinite-frequency case as a boundary value problem for Laplace's equation in two dimensions, the classic problem of inviscid flow around an impermeable obstacle (Keener 1988), or the elementary electrostatics problem of a thin grounded conductor (Panofsky & Phillips 1962). Once we have discovered the currents j_* we compute the conductance function via (32). The electric field on the conductors for finite ω follows as before from (29) and the electromagnetic fields can be extended out into the rest of space by the Biot-Savart law and analytic continuation. Thus any collection of thin conductors is a candidate for this treatment, but a potential impediment to its success is the requirement that τ be nonnegative. We call the family of successful thin conductors SR^+, for Single Resonance, Positive conductors.

We will illustrate the process with some examples. Consider some geometrical arrangement of thin conductors, which we will continue to call $\mathcal{C}$. We impose mirror symmetry across the line $z = 0$ as before to provide image currents that substitute for a perfect conductor on that line. The perfect conductor simplifies the analysis by providing a convenient boundary on which to set $E_y = 0$. For the purposes of producing some concrete examples it turns out to be more convenient to discard the integral equation formulation. The first step is to solve the boundary value problem in the limit $\omega \to \infty$.

As ω increases, E_y away from $\mathcal{C}$ grows indefinitely (in contrast to the field on $\mathcal{C}$ which remains finite), so we work instead with the magnetic field and its vector potential $\mathbf{A}$. Of course $\mathbf{B} = \nabla \times \mathbf{A}$ but, since we have a 2-D system, $\mathbf{A}$ possesses only one component $\mathbf{A} = \hat{\mathbf{y}}A$. We choose the gauge condition $\nabla \cdot \mathbf{A} = 0$ and then it is easily verified that in the interior $\nabla^2 A = 0$, that is, A is also a harmonic function. To match the driving magnetic field $A \to zB_0$ as $z \to \infty$. The condition that $B_n = 0$ on $\mathcal{C}$ means that $A =$ constant there. We may solve the boundary value problem by any of the standard methods, although the most useful to us is the application of complex analysis; see the next Section.

Once the solution for $\nabla^2 A = 0$ has been found, the next step is to calculate the current density in the thin conductor: by Ampère's law

$$\mu_0 j_* = \left(\frac{\partial A}{\partial n}\right)_+ - \left(\frac{\partial A}{\partial n}\right)_- \tag{33}$$

that is, the jump in normal derivative across the sheet. Thus we discover the lateral conductivity variation

$$\tau(s) = \frac{j_*(s)}{\varpi B_0 z(s)}, \tag{34}$$

where s is the distance along the curve of the conductor; recall ϖ is a free parameter. At this point we must check that $\tau \geq 0$.

If there are only positive values for τ we can proceed to solution of the TE mode induction problem at finite ω, as follows. Let $\mathbf{B}_*$ be the magnetic field associated with the current system j_* (not just on the conductor, but everywhere), easily found by $\mathbf{B}_* = \nabla \times \mathbf{A} - \mathbf{B}_0$. Then the magnetic field at frequency ω is the complex linear combination

$$\mathbf{B}(\omega) = \mathbf{B}_0 + \frac{\mathrm{i}\omega}{\varpi + \mathrm{i}\omega}\mathbf{B}_* \tag{35}$$

and similarly

$$-\frac{E_y(\omega)}{\mathrm{i}\omega} = zB_0 + \frac{\mathrm{i}\omega}{\varpi + \mathrm{i}\omega}A_*, \tag{36}$$

where $A_* = A - zB_0$ which is the y component of the vector potential associated with currents in $\mathcal{C}$. Evidently, these fields are associated with a single resonance at $\omega = \mathrm{i}\varpi$.

7 EXAMPLES

To generate examples we return to the representation of a harmonic function by an analytic function in the complex ζ plane. Our approach will be to begin with a vector potential and explore the shapes of the potential conductors $\mathcal{C}$ that arise from it. To solve the boundary value problem for Laplace's equation at infinite frequency we introduce a complex potential Ψ such that

$$A(x, z) = \mathrm{Re}\,\Psi(\zeta) = \mathrm{Re}\,\Psi(x + \mathrm{i}z). \tag{37}$$

From $\mathbf{B} = \nabla \times \mathbf{A}$ and (37) we find that

$$B_z(x, z) + \mathrm{i}B_x(x, z) = \frac{\mathrm{d}\Psi}{\mathrm{d}\zeta}. \tag{38}$$

Remember, in the limit $\omega \to \infty$, B_x and B_z are real: perfect conductors are not associated with phase shifts. The complex potential for the ribbon studied in Section 3 is

$$\Psi(\zeta) = -\mathrm{i}B_0\sqrt{\zeta^2 + a^2} \tag{39}$$

with the branch cut running directly between $\pm\mathrm{i}a$ where $\mathrm{Re}\,\Psi = 0$; the cut is identified with the conductor. In the following illustration we employ the classic potential associated with fluid passing over a hemicylindrical obstacle (Keener 1988):

$$\Psi(\zeta) = -\mathrm{i}B_0\zeta - \frac{\mathrm{i}B_0 a^2}{\zeta}. \tag{40}$$

As shown in Fig. 4 this function causes the contour $\mathrm{Re}\,\Psi = 0$ to form two parts, a circle of radius a centered on the origin and the line $z = 0$. The circle encloses the singularity. For the first illustration we will identify $\mathcal{C}$ with the zero-level contour. Then, because in the high frequency limit $\mathcal{C}$ becomes perfectly conducting, the magnetic field is excluded from the disc $|\zeta| < a$, shown shaded in the Figure. The vector potential inside is constant, and since A must be continuous, the constant is zero. Thus the solution to the boundary value problem for $\nabla^2 A = 0$ that we need is not the real part of Ψ in (40), but of

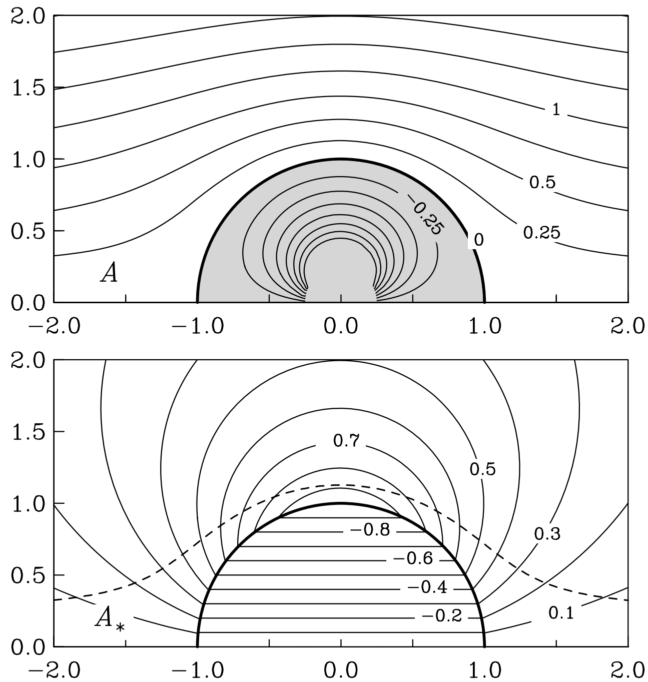

Figure 4. Top: contours of $\mathrm{Re}\,\Psi/aB_0$ given in (40). When the line $\mathrm{Re}\,\Psi = A = 0$ is chosen to be $\mathcal{C}$, the magnetic field at infinite frequency is excluded from the shaded region. Distances scaled by a. Bottom: scaled vector potential, $A_\star/aB_0$, associated with currents $j_\star$ flowing in $\mathcal{C}$.

$$\hat{\Psi}(\zeta) = \begin{cases} -\mathrm{i}B_0\zeta - \frac{\mathrm{i}B_0 a^2}{\zeta}, & |\zeta| \geq a \\ 0, & |\zeta| < a. \end{cases} \tag{41}$$

Contours of A are lines of force for $\mathbf{B}$; we show them in Fig. 4. The lower half of the Fig. 4 gives the vector potential A_* of the currents flowing in the conductor; A_* can be used with (35) and (36) to find the complete solution of the TE mode induction problem at any frequency.

To specify the conductivity and verify that it is a physically realizable model, we compute the normal derivatives of A and hence the current density j_*: $\hat{\Psi} =$ constant inside the disc, and therefore $(\partial A/\partial n)_- = 0$. Outside we observe that $(\partial A/\partial n)_+ > 0$ and so

$$\left(\frac{\partial A}{\partial n}\right)_+ = \left|\frac{\mathrm{d}\Psi}{\mathrm{d}\zeta}\right| = B_0\left|1 - \frac{a^2}{\zeta^2}\right|, \quad \zeta \in \mathcal{C} \tag{42}$$

$$= 2B_0 \sin\theta, \tag{43}$$

where $\theta = \arg\zeta$. Thus from (33) and (34) we find the conductance

$$\tau = \frac{2B_0 \sin\theta}{\mu_0 B_0 \varpi a \sin\theta} = \frac{2}{\mu_0 a \varpi} = \text{constant}. \tag{44}$$

There is no change of sign in τ so here is a new member of SR^+, a very simple one with constant conductance. In this case the conductance is bounded, unlike the behaviour we found in first solution, where $\tau(z)$ increases like $(a-z)^{-\frac{1}{2}}$ toward the tip of the conductor at $z=a$.

The choice of the contour $\mathrm{Re}\,\Psi=0$ in this example leads to a conductor of finite length, like the one which began our investigation. However, there is nothing special about that particular contour as far as the infinite-frequency boundary value problem is concerned: any line, $\mathrm{Re}\,\Psi=$ constant may serve as a potential conductor, since by definition $B_n=0$ on every one. If we choose a contour with $p=\mathrm{Re}\,\Psi<0$ we find $\mathcal{C}$ is one of the closed contours inside the shaded region. Those contours run right through the singularity at $\zeta=0$, and give rise to non-integrable current densities and a discontinuous vector potential. Such pathological behavior cannot be associated with a physical model.

In contrast, when we select a level with $\mathrm{Re}\,\Psi=p>0$ for $\mathcal{C}$, the normal derivatives of A and currents are well behaved. The conductor becomes infinitely long, a smooth symmetrical hummock that does not touch $z=0$ and which obeys the cubic equation

$$z^3-bz^2+(x^2-a^2)z-bx^2=0, \tag{45}$$

where $b=p/B_0$. The infinite-frequency boundary value problem has the solution $A=\mathrm{Re}\,\Psi$ above the curve, and $A=p$ below it. It is easily seen that, as before, $(\partial A/\partial n)_+>0$ and that (42) still applies, though not (43). Since $z>0$ everywhere on $\mathcal{C}$, we can construct a member of SR^+. For example, if we choose the line $p=\mathrm{Re}\,\Psi=0.25aB_0$, the new $\mathcal{C}$ becomes the line labelled 0.25 in the top half of Fig. 4, and dashed in the lower plot. The new $\mathbf{B}_*$ remains a dipole field above the dashed line, and the uniform magnetic field now fills the region below it. The current j_* sustaining A_* is shown in Fig. 5, along with the corresponding conductance of $\mathcal{C}$.

We must not leave the impression that every arrangement of thin conducting bodies leads to a member of SR^+ by the process of adjusting its conductance distribution. For example, consider a complex potential with two poles in the ζ plane:

$$\Psi(\zeta)=-\mathrm{i}B_0\zeta-\frac{\mathrm{i}B_0a^2\zeta}{\zeta^2+a^2} \tag{46}$$

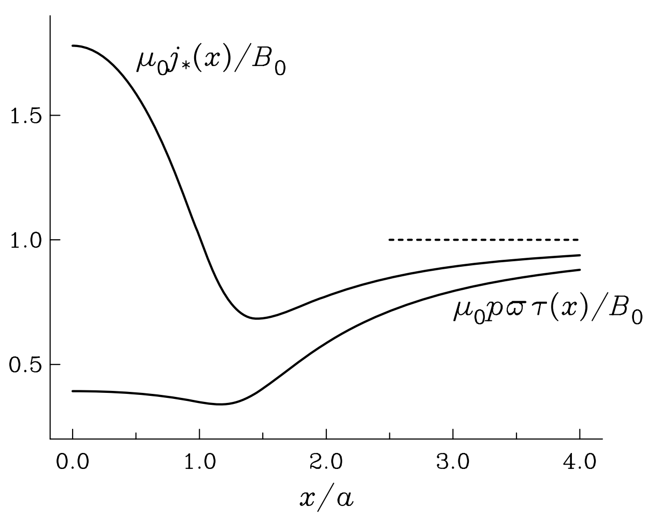

Figure 5. Current density $j_\star(x)$ in $\mathcal{C}$ shown in Fig. 4 when $p=0.25aB_0$ in the infinite-frequency limit, and corresponding conductance, $\tau(x)$. Quantities are scaled to be dimensionless.

which has the proper symmetry across $z=0$. If we choose for $\mathcal{C}$ the contour level $p=\mathrm{Re}\,\Psi=0.775702aB_0$ there is a closed, almost circular, oval which might be a member of SR^+. But to expel the source magnetic field at high frequency from the interior, current must flow in the conductor in both the positive and negative y directions, and hence negative τ is required in (34), making the model nonphysical.

For the purposes of creating a few simple examples we have chosen to start with Ψ and examine the shapes of potential members of SR^+. If, however, one wanted to specify the shape and to discover the associated complex potential, that boundary value problem could be solved by means of the Schwarz-Christoffel transformation (Driscoll & Trefethen 2002). We will not pursue that approach here.

8 DISCUSSION

We have described SR^+, a new class of special solutions to the TE mode MT problem in which the frequency response is remarkably simple: there is single pole on the imaginary frequency axis. The models are found by considering the infinite-frequency case of induction in an arbitrary arrangement of thin conductors, when the normal magnetic field vanishes on the conductors. Based on the currents in the system, we adjust the conductance distribution in the thin conductors appropriately. Many of these solutions can be written without approximation as finite expressions in elementary functions and therefore they are easily calculated and simple to analyze in detail. Singular models like these consisting of thin conducting layers, are natural models for a number of geophysically important systems, like fluid-filled cracks. Systems with a finite number of resonances play an important role in the 1-D MT inverse problem with finite data sets, but whether they are useful for inversion in two- and three dimensions is unknown.

This work leaves open a number of interesting questions. For example, How does one construct models with two resonant frequencies, or with N of them? The approach of this paper offers no clue. The only system with $N\geq 2$ resonances that the author has been able to devise is based on concentric cylinders, and there is no obvious path to greater generality. Another question is whether there are any models with a finite set of resonances for the transverse magnetic mode induction problem of MTs, where the driving magnetic field is parallel to the strike of the model. And of course, one must also wonder about fully 3-D systems. The analogous process in three dimensions to the one we have considered here leads to anisotropic conductance in the conducting sheets, because the electric current and the tangential electric field are vectors which will not in general be parallel. That seems to be an unnecessary complication. Clearly, we are far from a complete understanding of this unusual class of conductivity models.

ACKNOWLEDGMENTS

This work was supported in part by the Seafloor Electromagnetic Methods Consortium at Scripps Institution of Oceanography (http://marineemlab.ucsd.edu/semc.html); the author is particularly grateful to Steve Constable for his constant encouragement.
Thanks also to the Associate Editor for his insightful comments and to two anomymous reviewers for their close reading of the original manuscript.

REFERENCES

Driscoll, T.A. & Trefethen, L.N., 2002. *Schwarz-Christoffel Mapping,* Cambridge University Press, Cambridge.

Keener, J.P., 1988. *Principles of Applied Mathematics: Transformation and Approximation,* Addison-Wesley, Redwood City, CA.

Kellogg, O.D., 1953. *Foundations of Potential Theory,* Dover Publications, New York, NY.

Needham, T., 1999. *Visual Complex Analysis,* Oxford Univ. Press, New York, NY.

Panofsky, W.K.H. & Phillips, M., 1962. *Classical Electricity and Magnetism,* 2nd ed., Addison-Wesley, Reading, MA.

Parker, R.L. & Whaler, K., 1981. Numerical methods for establishing solutions to the inverse problem of electromagnetic induction, *J. geophys. Res.,* **86,** 9574–9584.

Parker, R.L., 1994. *Geophysical Inverse Theory,* Princeton University Press, Princeton, NJ.

Porter, D. & Stirling, D.S.G., 1990. *Integral Equations,* Cambridge University Press, Cambridge.

Weaver, J T., 1994. *Mathematical Methods for Geo-Electromagnetic Induction,* John Wiley and Sons, New York, NY.